

# Constitutively active ezrin increases membrane tension, slows migration, and impedes endothelial transmigration of lymphocytes in vivo in mice

Yin Liu,<sup>1</sup> Natalya V. Belkina,<sup>1</sup> Chung Park,<sup>2</sup> Raj Nambiar,<sup>3</sup> Scott M. Loughhead,<sup>4</sup> Genaro Patino-Lopez,<sup>1</sup> Khadija Ben-Aissa,<sup>1</sup> Jian-Jiang Hao,<sup>1</sup> Michael J. Kruhlak,<sup>1</sup> Hai Qi,<sup>5</sup> Ulrich H. von Andrian,<sup>4</sup> John H. Kehrl,<sup>2</sup> Matthew J. Tyska,<sup>3</sup> and Stephen Shaw<sup>1</sup>

<sup>1</sup>Experimental Immunology Branch, National Cancer Institute, Bethesda, MD; <sup>2</sup>Laboratory of Immunoregulation, National Institute of Allergy and Infectious Diseases, Bethesda, MD; <sup>3</sup>Department of Cell and Developmental Biology, Vanderbilt University Medical Center, Nashville, TN; <sup>4</sup>Department of Pathology, Harvard Medical School, Boston, MA; and <sup>5</sup>Laboratory of Immunology, National Institute of Allergy and Infectious Diseases, Bethesda, MD

**ERM (ezrin, radixin moesin) proteins in lymphocytes link cortical actin to plasma membrane, which is regulated in part by ERM protein phosphorylation. To assess whether phosphorylation of ERM proteins regulates lymphocyte migration and membrane tension, we generated transgenic mice whose T-lymphocytes express low levels of ezrin phosphomimetic protein (T567E). In these mice, T-cell number in lymph nodes was reduced by 27%. Lymphocyte migration rate in vitro and in vivo in lymph nodes decreased by 18% to**

**47%. Lymphocyte membrane tension increased by 71%. Investigations of other possible underlying mechanisms revealed impaired chemokine-induced shape change/lamellipod extension and increased integrin-mediated adhesion. Notably, lymphocyte homing to lymph nodes was decreased by 30%. Unlike most described homing defects, there was not impaired rolling or sticking to lymph node vascular endothelium but rather decreased migration across that endothelium. Moreover, decreased numbers of**

**transgenic T cells in efferent lymph suggested defective egress. These studies confirm the critical role of ERM dephosphorylation in regulating lymphocyte migration and transmigration. Of particular note, they identify phospho-ERM as the first described regulator of lymphocyte membrane tension, whose increase probably contributes to the multiple defects observed in the ezrin T567E transgenic mice. (*Blood*. 2012;119(2):445-453)**

## Introduction

Normal immune function depends on lymphocytes in circulation binding to vascular endothelium, transmigrating across the endothelium, and migrating within tissue.<sup>1-3</sup> Lymphocyte migration and transmigration depend on cytoskeletal reorganization, including especially the actin cytoskeleton. However, linkage between plasma membrane and actin cytoskeleton is a potentially important aspect, which has not yet been well studied. Ezrin-radixin-moesin (ERM) proteins are a trio of very closely related human paralogs whose primary function is mediating linkage between the plasma membrane and cortical actin, which is the shell of polymerized actin that lies just below the membrane.<sup>4,5</sup> One of the most fundamental aspects of ERM protein function is their ability to regulate that linkage by switching between active and inactive conformations. In the active conformation, the N-terminal region, the FERM domain, binds to plasma membrane lipids and cytoplasmic tails of transmembrane proteins and the C-terminal region binds to F-actin. However, in the dormant conformation, those 2 regions bind intramolecularly to each other and therefore cannot mediate linkage via intermolecular interactions. The conformational switch between dormant and active forms is initiated and sustained by ERM protein binding to PI(4,5)P<sub>2</sub> in the plasma membrane.<sup>4-7</sup> In addition, C-terminal phosphorylation plays an important role in stabilizing the active conformation. Solved structures of the dormant ERM protein elucidate the mechanism whereby phosphorylation stabilizes the active conformation. The critical threonine that is phosphorylated in ERM proteins (T567 in ezrin) is in the C-terminus close to

the interface involved in the autoinhibitory binding of the C-terminus to the FERM. T567 phosphorylation reverses the charge of that region and disrupts electrostatic interactions that normally promote autoinhibitory binding.<sup>4,5</sup>

ERM protein phosphorylation is dynamically regulated in many cell types in diverse physiologic contexts. Rapidly induced phosphorylation was first described by Furthmayr et al during thrombin activation of platelets.<sup>8</sup> Rapidly induced dephosphorylation was initially described in immune cells stimulated by soluble factors, such as chemokines that promote their recruitment from blood into tissue.<sup>9,10</sup> Because it is plausible that such regulated phosphorylation is functionally important in cellular processes, substantial investigation has been directed at establishing that connection. One of the most powerful approaches has been cell transfection with phosphomimetic mutant constructs of ERM proteins in which the phosphorylated threonine is replaced by a negatively charged residue to mimic phosphorylation.<sup>11</sup> Such phosphomimetic ERM proteins resemble normal active ERM in their enhanced localization at the plasma membrane in transfected cells.<sup>12</sup> They have been used in many biochemical and cell biologic studies of ERM protein activation/function to probe the roles of ERM phosphorylation/dephosphorylation.<sup>9,13-21</sup> For example, regulation of ERM protein phosphorylation has been implicated in functions as diverse as compaction in the mouse early embryo,<sup>14</sup> cell rounding in mitosis,<sup>21</sup> and promotion of uropod formation in lymphocytes.<sup>15</sup>

Submitted July 23, 2011; accepted November 12, 2011. Prepublished online as *Blood* First Edition paper, November 21, 2011; DOI 10.1182/blood-2011-07-368860.

The online version of this article contains a data supplement.

The publication costs of this article were defrayed in part by page charge payment. Therefore, and solely to indicate this fact, this article is hereby marked "advertisement" in accordance with 18 USC section 1734.

Importance of regulated ERM protein phosphorylation in 1 or more of the events involved in lymphocyte recruitment from blood into tissue was suggested by findings that a key trigger of this process (chemokines) induced rapid dephosphorylation of ERM protein. We hypothesized that ERM protein phosphorylation would regulate lymphocyte migration,<sup>9</sup> which is dependent on the cortical cytoskeleton and its interactions with the overlying plasma membrane. Several *in vitro* studies support the view that the presence of phosphomimetic ERM protein (ie, ERM protein unable to dephosphorylate) impairs lymphocyte migration.<sup>9,17,18</sup> However, apparently conflicting findings have been reported in 2 other studies.<sup>15,16</sup> Discrepancies between studies, which may reflect heterogeneity in cell types studied and in amounts of phosphomimetic ERM protein expressed, left ambiguity regarding the role of ERM protein phosphorylation in cell migration.

Membrane tension of the plasma membrane is, in effect, the resistance of the plasma membrane to deformation (resistance to a change in shape). Because many cellular processes involve deformation of the plasma membrane, theoretical considerations predict that membrane tension would regulate diverse cellular events occurring at the plasma membrane.<sup>22</sup> Although still limited in number, cell biologic investigations of membrane tension in eukaryotic cells suggest that membrane tension is a “master regulator” of many cellular processes.<sup>22-26</sup> Of likely relevance to cell migration, Sheetz et al provided evidence that lamellipod extension was negatively regulated by membrane tension.<sup>26</sup> The membrane tension of eukaryotic cell plasma membrane derives largely from the linkage of plasma membrane to the underlying cytoskeleton.<sup>22,27</sup> Only one family of molecules in eukaryotic cells has been shown to regulate membrane tension, namely, class I myosins.<sup>28</sup> We hypothesized that ERM proteins might also be involved in regulating membrane tension by virtue of their role, when phosphorylated/activated, in linking plasma membrane to actin cytoskeleton. While our studies were in progress, analysis of zebrafish mesoderm cells provided the first evidence that ERM proteins contribute to membrane tension.<sup>29</sup>

We generated transgenic mice expressing phosphomimetic ERM protein in lymphocytes to determine whether ERM protein phosphorylation regulates lymphocyte plasma membrane tension and downstream cellular functions, such as migration, which are expected to be controlled by this physical parameter. Ezrin and moesin, the 2 ERM proteins expressed in lymphocytes, have very high sequence similarity and are functionally interchangeable in many systems; we chose to study ezrin rather than moesin because some evidence indicates that ezrin has additional unique roles in lymphocytes.<sup>30,31</sup> Our results from these transgenic mice demonstrate that even a low level of phosphomimetic ezrin protein markedly elevates membrane tension and impairs lymphocyte migration. In addition, it impairs lymphocyte homing not by the usual mechanism of impaired intravascular adhesion to endothelium but rather by impairing transmigration.

## Methods

### Mice and cell culture

To generate ezrin transgenic mice, mouse ezrin mutant T567E cDNA was inserted into an hCD2-based mini-cassette. A hemagglutinin (HA) peptide sequence (YPYDVPDYA) was inserted at the C-terminus of the protein just before the stop codon. Transgenic mice were made and maintained on C57BL/6 background (National Cancer Institute). Control mice include both Ezrin wild-type (WT) transgenic mice made simultaneously and WT

C57BL/6 mice (littermates of the T567E transgenic mice). All mice used in the present study were housed in a specific pathogen-free facility and cared for in accordance with National Institutes of Health guidelines, and all protocols were approved by the National Cancer Institute Animal Care and Use Committee.

### Cell fractionation and Western blot

Primary T cells were purified from lymph node and spleen cells by removing B cells using Qiagen anti-mouse IgG magnetic beads. CD4<sup>+</sup> lymphoblasts were generated by selecting lymph node CD4 cells with anti-CD4 magnetic beads (Miltenyi Biotec) and activating them by plating  $2 \times 10^6$  per well in 6-well plates coated with 5  $\mu\text{g}/\text{mL}$  anti-CD3 antibodies. Three days later, the culture was fed with medium supplemented with IL-2 (Sigma-Aldrich; 50 U/mL) every other day. Before use, the cells were washed once and resuspended in HBSS (Sigma-Aldrich) with 2% FCS at  $10 \times 10^6$  per milliliter. Biochemical fractionation was done as previously described.<sup>7</sup> Western blot was performed using rabbit polyclonal anti-ezrin (Upstate Biotechnology), mouse monoclonal anti-ezrin pT567 (BD Bioscience), and monoclonal anti-Na/K-ATPase (Epitomics) using an infrared imaging system (Odyssey; Li-Cor Biosciences).

### SDF-1 stimulation-induced shape change

Freshly isolated lymphocytes were resuspended in HBSS containing 0.1% BSA (Sigma-Aldrich) and put on a rocker for 2 hours at 37°C for recovery. Then the cells were stimulated with SDF-1 (PeproTech) at a final concentration of 200 ng/mL at 37°C for the indicated time and the stimulation was terminated by mixing the cells with an equal volume of 4% paraformaldehyde. Cells were stained with phalloidin to detect F-actin and scored blind for polarization as described.<sup>9</sup> Images were acquired using Zeiss LSM510 Meta with a 40XC-apochromat (NA 1.2) water immersion objective lens. Image analysis was performed with Zeiss LSM 4.0 software. Anti-HA peptide tag mouse monoclonal antibody (Covance) was used to detect transgenic protein. For determination of asymmetry of transgenic protein localization within the cell, a binary image was created from the fluorescent image of anti-HA-stained cells and used to determine the cell outline and to calculate the cell center. A line was drawn through the center along the longest axis of the cell. The cell was bisected by creating a line through the center perpendicular to the long axis, and regions were created corresponding to each half. Those regions were applied to the original image to calculate mean pixel intensity in each half, and the ratio between back and front was calculated.

### Adhesion assay

The 96-well flat-bottomed plates were precoated with 5  $\mu\text{g}/\text{mL}$  of recombinant mouse ICAM-1/Fc or VCAM-1/Fc (R&D Systems) or 2% BSA as a control. Cultured T lymphoblasts were washed 3 times with PBS, resuspended in PBS at  $1 \times 10^6$  cell/mL, and labeled with 5  $\mu\text{g}/\text{mL}$  7-bis (2-carboxyethyl)-5-(and-6) carboxyfluorescein for 30 minutes at 37°C and washed 3 times with HBSS media containing 1mM HEPES, 0.1% BSA, 1 mM CaCl<sub>2</sub>, 1mM MgCl<sub>2</sub>, with or without 1mM MnCl<sub>2</sub>. A total of  $0.5 \times 10^5$  labeled cells were plated into each precoated well, and the plates were incubated at 37°C for 25 minutes. The wells were washed vigorously 3 times with the aforementioned HBSS buffer and the remaining adherent cell number assessed using a fluorescence microplate reader (Bio-Tek) using excitation and emission wavelengths of 485 and 528 nm.

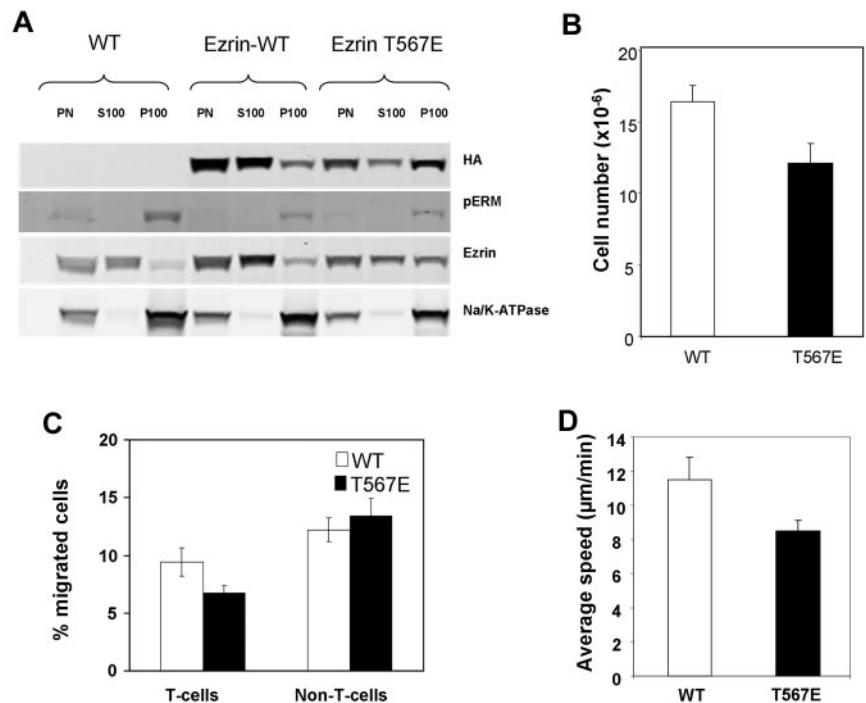
### Transwell assay

The transwell assay was done as previously described<sup>17</sup> using 3- $\mu\text{m}$  pore size transwells. Cells ( $2-10 \times 10^6$ ) were placed in the upper chamber of the transwell; the lower chamber was filled with RPMI 1640 with 400 ng/mL SDF-1 and 0.2% BSA. After 2 hours at 37°C, cells were collected and counted using fluorescent beads as a standard (Caltag/Invitrogen) on a FACSCalibur (BD Biosciences).

### In vitro migration assay

T lymphoblasts ( $1 \times 10^6$ ) were added to a MatTek dish in which the center well was coated with ICAM-1 (10  $\mu\text{g}/\text{mL}$ , 37°C for 1 hour) and filled with

**Figure 1. Initial characterization of ezrin transgenic mice.** (A) Assessment of ezrin localization at the plasma membrane. Purified peripheral T-lymphocytes were sonicated, the nuclei and cellular debris were removed by centrifugation, and the postnuclear fraction (PN) was separated by ultracentrifugation into the soluble fraction (S100, cytosolic) and the pellet (P100, containing plasma membrane). Samples resolved by SDS-PAGE were analyzed by Western blot with antibodies to HA (to detect transgenic ezrin), to pERM (to detect endogenous phosphorylated ERM; note that this antibody does not detect the T567E ezrin), to ezrin (to detect endogenous and transgenic ezrin), and to Na/K ATPase (to assess plasma membrane enrichment in P100). Note that loading for the P100 fraction was 6 times that of the PN and S100 fractions ( $18 \times 10^6$  vs  $3 \times 10^6$  cell equivalents) to assure sensitive detection of protein localization there. (B) Lower T-lymphocyte number in lymph nodes in T567E mice ( $P < .05$ ). Data are mean  $\pm$  SE of the number of T cells recovered from cervical, axillary, inguinal, lumbar, and mesenteric lymph nodes of 7 individual mice. (C) Reduced *in vitro* lymphocyte transmigration in T567E mice ( $P < .05$ ). Primary splenic lymphocytes ( $20 \times 10^6$ /mL) were incubated in the upper chamber of transwell chambers with 3- $\mu$ m polycarbonate membranes, and the number of cells transmigrated to the lower chamber containing 400 ng/mL SDF-1 was assessed after 2 hours by flow cytometry. Data are mean  $\pm$  SE of transmigration results for 7 T567E mice and 5 WT mice assessed in 4 separate experiments. (D) Slower migration rate of CD4 T-lymphoblasts from T567E mice ( $P < .0001$ ). Migration was assessed on an ICAM-1-coated surface. Data are mean  $\pm$  SE of values for 72 WT and 80 T567E cells in 3 separate experiments.



2% FCS HBSS. The cells were allowed to settle for 5 minutes, the unattached cells were gently washed off, and the dish was filled with approximately 2 mL 2% FCS HBSS. Live cell time-lapse images were acquired using a Zeiss Axiovert 200M microscope equipped with a 20 $\times$  (NA 0.8) plan-apochromat objective lens, differential interference contrast optics, a Photometrics Coolsnap ES CCD camera, and Axiovision Version 4.8 image acquisition software. Image analysis was performed using the Track Objects module of Metamorph Version 7.7 software. Briefly, regions of interest were placed around each cell in the initial image frame in the time series and followed through the subsequent image frames. The position coordinates for each cell were recorded, and the cell migration speed was calculated.

### Statistics and reproducibility

*P* values were calculated with unpaired *t* test or Mann-Whitney test by GraphPad Prism. Each figure represents data on at least 2 representative independent experiments.

### Measurement of membrane tension, *in vivo* homing, and intravital microscopy

Measurement of membrane tension, *in vivo* homing, and intravital microscopy are described in supplemental Methods (available on the *Blood* Web site; see the Supplemental Materials link at the top of the online article).

## Results

### Generation of transgenic mice expressing ezrin T567E in T-lymphocytes

Ezrin transgenes were expressed under the control of a human CD2 mini-cassette to restrict expression primarily to T-lymphocytes. The mutant construct incorporated a T567E mutation that mimics activation by phosphorylation and was C-terminally tagged with a peptide hemagglutinin tag (with less potential for altering ERM function than the larger GFP tag). For control purposes, transgenic mice expressing the corresponding construct without the T567E

mutation were also generated. To maximize physiologic relevance, we selected transgenic lines in which ezrin T567E protein was expressed at levels about half that endogenous ezrin in normal resting lymphocytes (supplemental Figure 1). Because the WT ezrin transgene was expressed at lower levels than ezrin T567E, homozygous WT ezrin transgenic mice were used since their protein expression was minimally greater than in the ezrin T567E heterozygotes. Selective expression of the transgenes in T-lymphocyte was evident, for example, in their expression in T-lymphocytes rather than B-lymphocytes (supplemental Figure 2).

One of the cardinal features of activated ERM protein is localization at the plasma membrane, in contrast to autoinhibited ERM protein that is primarily cytosolic. We assessed membrane localization of the ezrin T567E transgenic protein in primary lymphocytes by biochemical fractionation because their scant cytoplasm makes immunofluorescent assessment of membrane localization difficult. The results (Figure 1A) demonstrate that much of the transgenic ezrin T567E protein is present in the membrane fraction. In contrast, little of the WT ezrin transgenic protein is found there. This behavior of transgenic protein mimics the behavior of endogenous ezrin protein, the majority of which is cytosolic (ezrin blot), but the phosphorylated subset of ERM proteins is predominantly at the membrane (pERM blot). Biochemical fractionation of primary short-term cultured lymphoblasts also confirmed that ezrin T567E preferentially localized at the plasma membrane in such cell preparations (data not shown).

We investigated whether there were any major abnormalities in the development of T-cell lineage cells or in their steady-state distribution within lymphoid tissue in ezrin T567E transgenic mice. Analysis of thymocytes showed that positive selection, as identified by cells coexpressing CD69 and TCR $\beta$ , was intact as was generation of mature CD4 and CD8 cells (supplemental Figure 3A). In the periphery, the distribution between CD4 and CD8 subsets in lymph node was within the normal range (supplemental Figure 3B) and CD5 expression (investigated as an activation



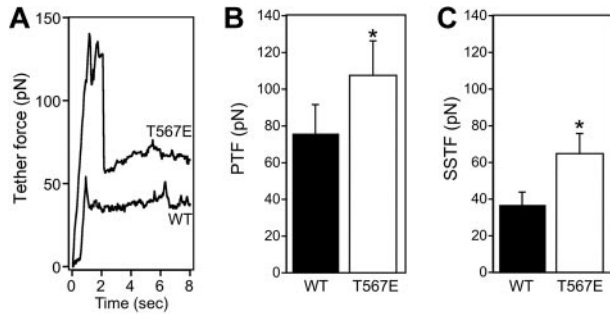


**Figure 2. Ezrin T567E transgenic lymphocytes have increased membrane tension.** (A) Representative single tether force traces are shown for WT and ezrin transgenic T567E T-cell blasts. (B-C) Bar graphs showing mean  $\pm$  SE of the PTF and the SSTF from WT (solid fill) and T567E (white fill) T-cell blasts. (WT PTF,  $75.9 \pm 15.7$ ; WT SSTF,  $36.8 \pm 7.1$ ; T567E PTF,  $107.8 \pm 18.5$ ; T567E SSTF,  $64.8 \pm 10.9$ ). \*Populations are significantly different ( $P < .05$ ). The PTF represents the force required for successful formation of a membrane tether. The PTF has a small contribution from the force required to overcome the membrane's resistance to a change in shape and a larger contribution from the force required to break membrane-cytoskeleton adhesion bonds.<sup>32</sup>

marker) was not changed (supplemental Figure 3C). However, T-cell number was somewhat reduced in lymph nodes in ezrin T567E transgenic mouse ( $\sim 27\%$ , Figure 1B). We therefore investigated whether transgenic T cells had alterations in migration and in homing that could contribute to this phenotype.

#### Abnormalities in T-lymphocyte migration in vitro

Our initial studies assessed lymphocyte migratory responses to chemokines in transwell chambers (Figure 1C). The percentage of ezrin T567E splenic T cells migrating was markedly reduced relative to littermate controls. In contrast, the percentage of splenic non-T cells that migrated was equivalent between the transgenic and controls; thus, impairment of migration was restricted to the lymphocyte population in which the transgenic protein was expressed. The transmigration assay is especially complex, including chemokine-mediated activation, adhesion, shape change, and migration. To assess whether migration per se is impaired, we assessed migration speed in a model system in which migration is spontaneous, rather than chemokine-induced. Migration of lymphoblasts on ICAM-1-coated surface was recorded and the migration paths analyzed (Figure 1D). Migration rate of ezrin T567E transgenic T cells was 18% slower than WT ezrin transgenic T cells.

#### Analysis of molecular processes that could impair migration

We investigated plasma membrane tension, which is increasingly viewed as a master regulator of many cellular processes that involve membrane deformation, including cell migration. Membrane tension is measured in an optical trap assay in which a thin membrane tether ( $\sim 100$ -nm diameter) is pulled from the cell surface and the required forces are measured corresponding to the peak during initiation of the tether (peak tether force [PTF]) and the steady state for tether maintenance at a constant length (steady-state tether force [SSTF]; Figure 2). The forces measured in WT lymphoblasts ( $36.8$  pN SSTF,  $75.9$  pN PTF) are at the very high end of diverse cell types previously studied using similar methods. For example, intestinal epithelial cells and fibroblasts exhibit SSTF values of approximately  $35$  pN and  $8$  pN, respectively, and PTF of approximately  $60$  pN and  $10$  pN, respectively. There are no comparable studies of membrane tension in other hematopoietic cells, but measurements in neutrophils using different technology measured a "cross-over force" (which may be functionally similar to our

measurement of PTF) of approximately  $40$  to  $50$  pN.<sup>33</sup> A marked increase in membrane tension was observed in the ezrin T567E transgenic lymphocytes. Representative single traces (Figure 2A) illustrate that T567E transgenic cells require a higher force for tether formation (PTF) and for tether maintenance at a constant length (SSTF). Statistical analysis of populations of cells confirms that PTF is 21% greater in the T567E transgenic cells than in WT cells (Figure 2B). SSTF, which is directly related to apparent membrane tension,<sup>34</sup> is increased by 71% (Figure 2C).

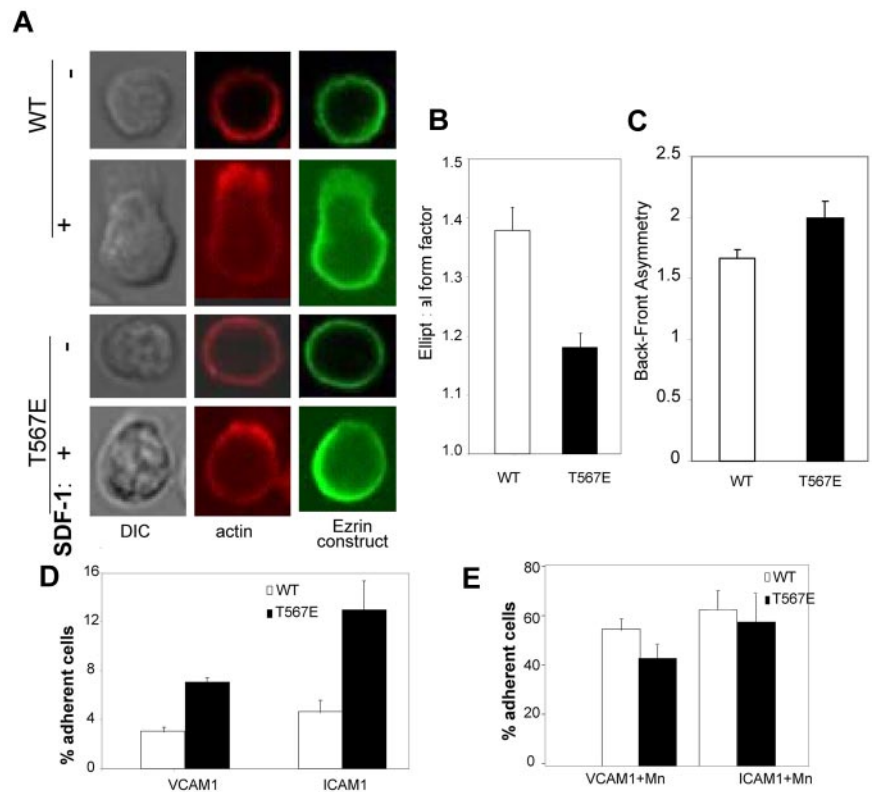
Because shape change is essential to migration, we analyzed T-cell shape change in response to chemokine stimulation. Resting primary T cells have a characteristic spherical morphology with cortical F-actin uniformly distributed at the plasma membrane; this morphology is shared by WT and ezrin T567E transgenic cells (Figure 3A-B). Within 1 minute after chemokine stimulation, the majority of WT cells become polarized with substantial depolymerization of the cortical F-actin in most areas of the cell and the striking extension of a lamellipod driven by localized actin polymerization. The ezrin T567E transgenic cells also generally polarized their F-actin at one pole of the cell but showed much more limited extension of lamellipods. To objectively score shape change, we used the parameter "elliptical form factor," which equals 1.0 for a circle and becomes progressively larger as cells become elongated (Figure 3B). Change in ezrin T567E transgenic cell shape was about half that of WT cells ( $\Delta$ shape index =  $0.18$  vs  $0.37$ ). WT transgenic ezrin protein was preferentially localized at the trailing edge of the T cells, but transgenic T567E ezrin was significantly more asymmetric in its distribution (Figure 3C). These findings are consistent with the preferential localization of ERM protein in the uropod, especially phospho-ERM.<sup>15,35</sup>

Finally, we analyzed static adhesion of T lymphoblasts to immobilized ligands ICAM-1 and VCAM-1 (Figure 3D), which could influence migration. Adhesion of the T567E transgenic T cells was consistently greater than WT cells to both ICAM-1 and VCAM-1 in the absence of  $Mn^{2+}$ . Note that adhesion of ezrin T567E T cells was similar to WT cells in the presence of  $Mn^{2+}$  (Figure 3E), which activates integrin-mediated binding by inducing a conformational change in those molecules. Because levels of expression of the adhesion receptors (LFA-1, VLA-4) are equivalent in both cell types (supplemental Figure 4), the augmented adhesion in the absence of  $Mn^{2+}$  apparently reflects an increase in integrin-mediated adhesion (eg, because of altered affinity or altered cytoskeletal linkage), not increased expression of integrins.

#### Slower T-lymphocyte migration in vivo

To ascertain whether slower migration was also evident in vivo, migration was assessed by 2-photon microscopy in lymph node. To achieve a well-controlled comparison of ezrin T567E transgenic T cells with controls, the 2 cell populations were stained with different dyes, coinjected intravenously, and their migration in lymph node cortex assessed approximately 18 hours later. Paths of WT (red) and T567E transgenic (green) cells in deep T-cell cortex were analyzed (Figure 4A-C). Migration of T567E transgenic cells was 20% slower than WT cells analyzed concurrently. Because there are some differences in tissue organization of different subregions of the T-cell area of lymph nodes, we analyzed separately migration in cortical subregions close to B-cell follicles. In those areas (Figure 4D-F), the decrease in migration speed of T567E transgenic cells was even more pronounced (47% decrease).

**Figure 3. Adhesion and shape change.** (A) Shape change of representative primary CD4 T cells before (–) or 60 seconds after (+) SDF-1 stimulation. Midplane confocal images stained for actin (phalloidin, red) and for the transgenic protein (using anti-HA, green). (B) Scoring of populations of cells from panel A (n = 30) for their shape 5 minutes after SDF-1 stimulation. Because the elliptical form factor scores = length of longest axis/length of axis perpendicular to that, a value of 1.0 is a round cell, and higher values are progressively more elliptical ( $P < .001$ ). (C) Analysis of asymmetry of transgenic protein. Lymphocytes were stimulated with SDF-1 and stained with anti-HA to detect localization of WT or T567E transgenic protein. For each cell, average pixel intensity was compared between the front and the back. Data are the mean  $\pm$  SE of values for 70 cells each ( $P < .05$ ). (D-E) Adhesion of CD4 T-lymphoblasts to immobilized VCAM-1 or ICAM-1 in the absence (D) or presence (E) of  $Mn^{2+}$ .



**Defective homing but normal binding to endothelium**

The reduction in number of T cells in lymph nodes of T567E transgenic mice (Figure 1B) raised the possibility that lymphocyte recirculation might be impaired. We assessed homing of T cells to lymph node by intravenous adoptive transfer of a mixture of T567E transgenic and WT lymph node cells followed by measurement of the number found in lymph node and blood. There was a 30% reduction in the number of T567E transgenic T-lymphocytes in lymph node after 1 hour and a corresponding increase of those cells in blood (Figure 5A). In contrast, non-T cells from T567E transgenic and WT mice were equivalent in lymph node and blood. Two possible explanations for impaired homing were considered first: altered microvilli<sup>9</sup> or reduced

expression of adhesion molecules involved in homing/recirculation. Scanning electron microscopy did not identify any apparent alteration in microvilli in T567E transgenic T cells (supplemental Figure 5). Surface expression of the relevant integrins was not reduced (supplemental Figure 6). However, inconsistently, a small reduction in CD62L was identified on T567E transgenic CD4 T cells. Its significance was unclear because CD62L is easily shed by protease cleavage,<sup>36</sup> but it raised the possibility of a resulting defect in rolling.

We therefore analyzed in vivo the lymphocyte-endothelial adhesion cascade whereby T-lymphocytes bind to lymph node vascular endothelium. Labeled T cells were injected into the arterial system of a mouse and lymphocyte adhesion imaged during

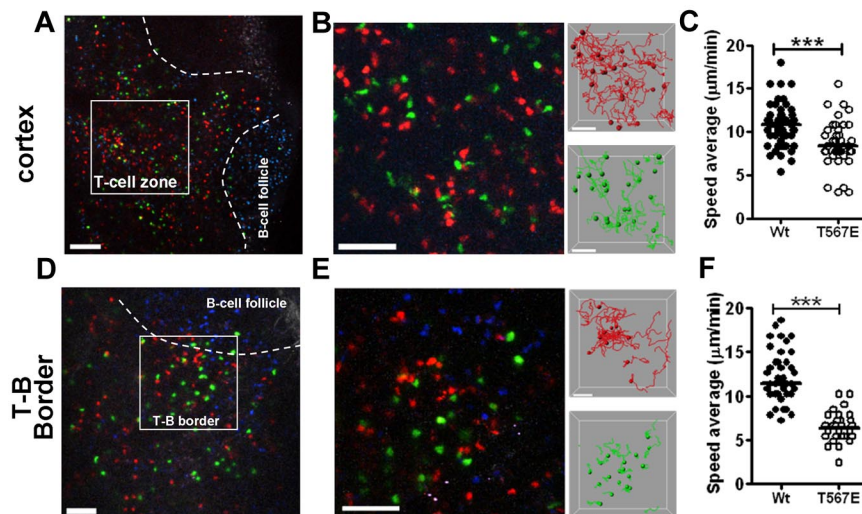


**Figure 4. Slower migration of ezrin T567E transgenic T cells in lymph node in vivo.** One day before imaging, WT B-lymphocytes, which were stained with blue (CMF<sub>2</sub>HC), were injected to delineate B-cell follicles. T-lymphocytes from WT mice were stained red (CMTMR) and from ezrin T567E transgenics were stained green (CMFDA), mixed, injected intravenously, and migration in inguinal lymph node was assessed 18 hours later by 2-photon microscopy. (A) Image of region of central T-cell cortex marking representative region for analysis. Bar represents 100 μm. (B) Frame from region analyzed along with tracks of WT (green) and ezrin T567E transgenic (red). Bar represents 30 μm. (C) Summary of migration speed of individual cells shows lower average speed of ezrin T567E transgenic lymphocytes ( $P < .0001$ ). Data are mean  $\pm$  SEM: WT (10.8  $\pm$  0.3 μm/s; N = 55), Tg (8.7  $\pm$  0.4 μm/s; N = 40). (D-F) Comparable analyses of migration near the border between T-cell area and B-cell follicle. Migration speed mean  $\pm$  SEM: WT (12.2  $\pm$  0.5 μm/min; N = 39), Tg (6.4  $\pm$  0.3 μm/min; N = 30). All  $P$  values were calculated using the Mann-Whitney test in Prism Version 5 (GraphPad). \*\*\* $P < .0001$ .

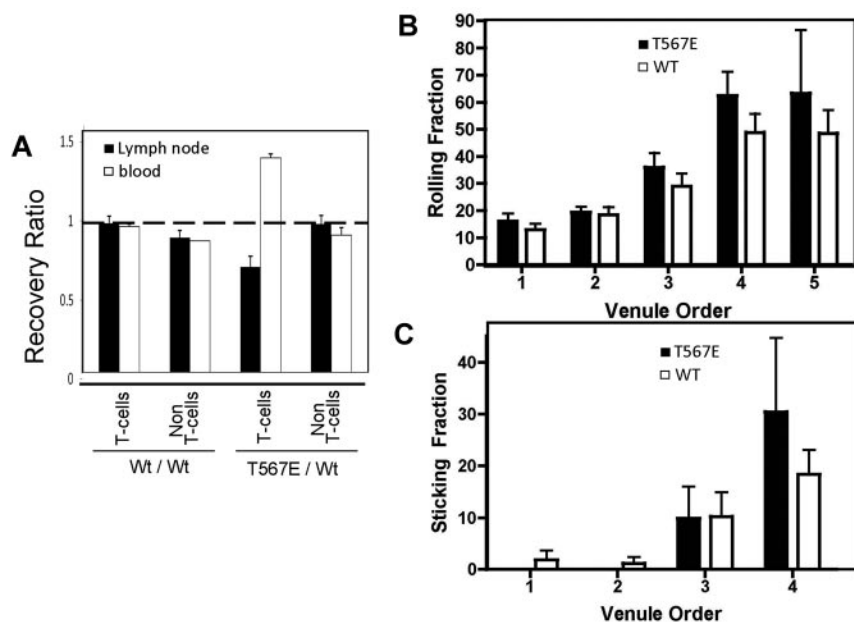


**Figure 5. Impaired homing of ezrin T567E transgenic T cells to lymph node.** (A) In vivo homing to lymph node. To assess homing in an internally controlled manner, 2 different T-cell preparations were stained with different levels of CFDA, mixed, injected intravenously, and their recovery in lymph node and blood was assessed by flow cytometry after 1 hour. Data are mean  $\pm$  SEM for pairs of mice in an experiment representative of 4 performed in which the experimental mix (right side of panel) was ezrin T567E transgenic cells and WT cells. The control mix (left side of panel) was WT cells and WT cells. Recovery ratios for the control mix were all close to 1.0 (dashed horizontal line). In the experimental mix, the recovery ratio was decreased for transgenic T cells in lymph node ( $P < .05$ ) and increased in blood ( $P < .01$ ), but recovery ratios close to 1.0 were observed for the non-T cells. (B) Assessment of lymphocyte rolling in inguinal lymph node. Lymph node T cells were injected intra-arterially, and the number showing slow movement characteristic of rolling during the first pass through the lymph node was scored blind. The venule order designations were assigned by counting successive generations of venular branches in the upstream direction from the large collecting venule that drains into the superficial epigastric vein (with first being the largest and fifth being the smallest). (C) Same as in panel B but showing assessment of the fraction of rolling cells that bind for more than 30 seconds.

their first pass through lymph node high endothelial venules (HEVs). Video recordings were analyzed to score the fraction of lymphocytes that rolled on lymph node vascular endothelium (Figure 5B) and the fraction of rolling lymphocytes that transitioned to stable binding (Figure 5C). No defect was identified in either rolling or stable binding.

#### Defective entry and exit from lymph node

The lack of a defect in rolling or firm adhesion was notable because most of the described defects in homing are caused by impairments in these steps. We reasoned that the defect could reflect a disability of adherent T567E transgenic lymphocytes in entering into the lymph node. We therefore analyzed events that follow lymphocyte adhesion to lymph node endothelium, with special attention to their persistence in the vessel and/or their transmigration across the endothelial well into the lymph node parenchyma. To unambiguously view the vessel boundary, HEVs were stained by a low concentration of fluorescence-labeled MECA-79 (Figure 6A). This allowed visualization of cell migration in the lumen followed either by transmigration into parenchyma or disappearance, apparently by de-adhesion (Figure 6B; supplemental Video 1). Approximately 80% of WT cells that bound to the HEVs went on to transmigrate, but only 50% of T567E transgenic cells did so (Figure 6C). Moreover, the T567E transgenic cells that did transmigrate took about twice as long to do so as WT cells (Figure 6D).

It was paradoxical that the rate of entry of T567E transgenic cells into lymph node was reduced but that the number of T567E transgenic cells in parenchyma was similar to that of WT cells at 24 hours. We therefore considered the possibility that T567E transgenic cells might also have impaired egress from lymph node. Findings of cell frequency in efferent lymph provided support for that hypothesis. The frequency of WT cells within the sinus was several-fold higher than T567E transgenic cells (Figure 6E), even though these cells were about equally represented in the lymph node cortex (Figure 6F).

## Discussion

The foregoing studies demonstrate that expression of mutant ezrin protein mimicking phosphorylated ezrin results in substantial impairment of lymphocyte entry into (and exit from) lymph node and their migration within it. These findings provide a strong teleologic explanation why chemokines induce rapid ERM dephosphorylation because they are prototypic stimulators of lymphocyte recruitment into lymph node.<sup>9</sup> The discussion focuses on the following: (1) why functional changes are observed despite the relatively low level of expression of phosphomimetic ezrin; and (2) the contribution of phospho-ERM to membrane tension and related stiffening mechanisms, and their ability to influence lymphocyte transmigration and migration.

#### Limited increase in active ERM protein has functional consequences

An increase of active ezrin (transgenic phosphomimetic ezrin) at the membrane impairs lymphocyte shape change (Figure 3), slows down lymphocyte migration (by 18% in vitro and 20%-47% in vivo; Figures 1 and 4), and impairs lymphocyte entry into lymph node after binding to endothelium (by 30%; Figure 5). The implication of these findings is that processes/pathways that regulate ERM protein phosphorylation state must be precisely regulated. These results confirm predictions that ERM dephosphorylation is important to facilitate shape change, transmigration, and migration.<sup>9</sup> In contrast, the present findings do not confirm a separate prediction that ERM dephosphorylation might promote collapse of microvilli<sup>9</sup> because T567E transgenic lymphocytes showed no augmentation of microvilli, no consistent delay in microvilli resorption after chemokine stimulation (supplemental Figure 5), and no defect in sticking to endothelium (Figure 5). Perhaps the low level of expression of the transgene in the transgenic model explains the absence of an effect on microvillus collapse.

Of particular note is the impaired transmigration across vascular endothelium (Figure 6). There is limited precedent for this kind of



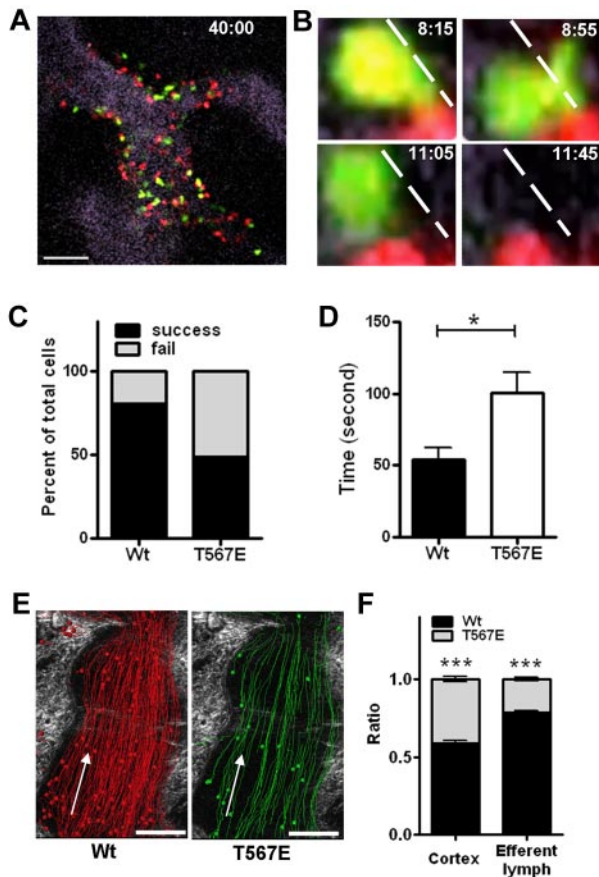


**Figure 6. Defect in entering and leaving lymph node.** (A-D) Imaging of events at the endothelial interface in lymph node. HEVs were stained by a low concentration of fluorescence-labeled MECA-79 (visualized as gray). T-lymphocytes from WT mice were stained red (CMTMR) and from ezrin T567E transgenics were stained green (CMFDA), mixed and injected intravenously while inguinal lymph node was being imaged at frame rate of 5 seconds. (A) A representative still image of HEVs showing lymphocytes at the endothelial surface and in the immediate vicinity of the vessel 40 minutes after cell injection. (B) Four sequential still images with corresponding time stamp. Dashed line indicates the edge of vessel delineated by MECA-79 stain, which is better seen on lower magnification view. Sequence illustrates an ezrin T567E transgenic T-cell initiating transmigration (maximal at 8:55), then withdrawing extension (11:05) and de-attaching (11:45). (C) Scoring of the success or failure of WT or T567E transgenic T-lymphocytes to transmigrate from endothelium into interstitium. (D) Average time taken for lymphocytes to transmigrate ( $P = .0185$ ). Data are mean  $\pm$  SEM: WT ( $53.9 \pm 8.2$ ;  $N = 9$ ), Tg ( $100.6 \pm 14.1$ ;  $N = 16$ ).  $P$  values were calculated with Mann-Whitney test by Prism Version 5 (GraphPad).  $*P < .05$ . (E) Thirty minutes of cumulative image of cell movement in representative lymph node in efferent lymph. Arrow indicates direction of lymph flow. (F) Comparison of the relative number of lymphocytes of ezrin T567E versus WT-lymphocytes from panel E in cortical sinus compared with cortex.  $***P < .01$ .

transmigration defect in contrast to more frequently described defects in rolling or strong adhesion. The most relevant precedents are demonstrations that hematopoietic cells unable to properly down-regulate LFA-1 or  $\alpha 4/\beta 7$  affinity had impaired migration into peritoneum or lymphoid tissue.<sup>37-39</sup> One study documented perturbed intravascular crawling of such cells to transmigration sites and compromised diapedesis across endothelium.<sup>37</sup> Could alterations in integrin regulation contribute to the defects in our model because we observed a modest increase in adhesion to ICAM-1 and VCAM-1? Possibly, but multiple differences suggest that is not the primary mechanism in our model. Unlike the findings in models with altered integrin affinity regulation, (1) our transgenic lymphocytes did not display a huge increase in sticking fraction (compare with  $\sim 4$  times increase with integrin alterations<sup>37,39</sup>); (2) our transgenic lymphocytes lost their adhesion

difference in the presence of  $Mn^{2+}$  (Figure 3C); and (3) impaired polarization was observed in ezrin T567E transgenic lymphocytes in an anchorage independent assay, in which integrin adhesion is not involved (Figure 3A-B). At some level, the finding that our transgenic lymphocytes “fall off” endothelium resembles the defect observed in knockout mice lacking signaling molecules, such as PI-3K,<sup>40</sup> Vav-GEFs,<sup>41</sup> and Syk.<sup>42</sup> However, it differs fundamentally because those models have not had associated impairment of recruitment into tissue<sup>41,42</sup> and because our lymphocytes have prolonged transit time in moving across endothelium (Figure 6D).

The present results strongly argue that regulated ERM phosphorylation is critical for lymphocyte migration and transmigration. They substantially address 3 key previous concerns. First, our transgenic cells have documented low level expression of the phosphomimetic protein (supplemental Figure 1), unlike the uncharacterized expression levels in cells used in previous potentially contradictory studies.<sup>15,16</sup> Second, previous studies have used a single in vitro model, transmigration in transwell chambers.<sup>15,16</sup> In contrast, we have dissected components of that complex response and extended the analysis to multiple in vivo functional assays (Figures 4-6). Third, to maximize physiologic relevance, we have used primary lymphocytes, unlike a previous study of spontaneously polarized tumor cells EL4 cells.<sup>15</sup>

### Membrane tension

The large literature on ERM proteins demonstrates that they participate in many cellular and molecular processes.<sup>4,5,43</sup> This is perhaps predictable because: (1) ERM proteins are among the most abundant cytosolic proteins in lymphocytes<sup>44</sup>; (2) ERM proteins bind to more than 50 different binding partners; and (3) binding occurs via 4 well-defined binding sites and many other proposed regions. Therefore, it is not surprising that multiple mechanisms (Figures 2 and 3) might contribute to the impairment of migration and transmigration in ezrin T567E transgenic lymphocytes.

In these studies, we identify a new mechanism by which ERM proteins may regulate shape change and migration, namely, by controlling membrane tension. Membrane tension in the ezrin T567E lymphocytes is increased by 71% relative to controls cells. Our results confirm the recent studies of Diz-Munoz that ERM protein positively regulates membrane tension<sup>29</sup> and extend them by implicating the phosphorylated form in mediating this function. An increase in membrane tension would be predicted to impair lamellipod extension based both on theoretical considerations and on experimental data.<sup>26</sup> Because membrane tension opposes protrusion of the lamellipod, an increase in membrane tension would be predicted to make it harder for cells to extend a lamellipod, which has been confirmed experimentally in fibroblasts.<sup>26</sup> The phenotype of ezrin T567E lymphocytes undergoing chemokine-induced polarization resembles that predicted for cells with increased membrane tension: actin polymerization at one pole, but ineffective lamellipod extension at that pole (Figure 3).

ERM proteins (especially phospho-ERM) enhance cellular resistance to shape change as measured in 3 distinct assays: measurement of (1) membrane tension, (2) cortical tension, and (3) global cell deformability. First, low levels of phospho-ERM markedly increase membrane tension (Figure 2). Second, Baum et al reported increased cortical tension in *Drosophila*-cultured S2R cells during mitosis and after transfection with phosphomimetic moesin.<sup>21</sup> Third, Delon et al reported that transfection of lymphocytes with a dominant negative ERM construct reduces lymphocyte resistance to global deformation.<sup>45</sup> These 3 assays measure attributes of stiffness that are distinct but related. Cortical tension is a

measure of the local deformability of the cytoskeleton immediately below the plasma membrane (especially actin-based cortical cytoskeleton in lymphocytes); it is measured by assessing how much force is required to indent a local area of the cell. Membrane tension (assessed by pulling a membrane tether) measures the in-plane stiffness of a membrane bilayer, but a dominant determinant of it is the physical connections between the cytoskeleton and the overlying plasma membrane.<sup>29,32</sup> Global cell deformability is a more inclusive measurement, which includes both of the previous parameters as well as nuclear deformability; it is measured by determining how much a whole cell is deformed by a distributed force (such as centrifugation). Because these 3 parameters are inter-related, we cannot conclude that defects in transmigration and migration in these transgenic lymphocytes are uniquely caused by isolated changes in any one of them. Rather, we hypothesize that there is cooperativity among these mechanisms. For example, an increase in the connection between membrane and cortex in the presence of phospho-ERM (measured by membrane tension) probably promotes recruitment and enhancement of cortical cytoskeleton (which is measured by cortical tension).

There are additional complexities that are only partially understood regarding the relationship between phospho-ERM and migration. For example, that relationship depends on the cell type studied, apparently at least partly attributable to the mode of migration those cells use. In contrast to lymphocytes, which use lamellipod extension to migrate other cell types, such as primordial germ cells in zebrafish and some cancers cells, migrate using bleb-like protrusions.<sup>46</sup> Knockdown of ERM protein in zebrafish decreased membrane tension of mesoderm and increased bleb formation (as predicted). However, it did not alter their instantaneous rate of migration.<sup>29</sup> Unexpectedly, it decreased their straightness of migration; the mechanism was speculated to relate to alterations in protrusion types. A recent report may help explain the zebrafish results because it found that ERM protein enrichment in the uropod contributed to directional control of certain kinds of bleb-dependent migration.<sup>47</sup> In our lymphocytes, the phosphomimetic ezrin was preferentially localized in the rear of the cell (Figure 3C), but its presence did not enhance the straightness of migration in vitro of lymphocytes (which is not dependent on blebs; data not shown). Such uropod enrichment of phosphomimetic ezrin in transgenic lymphocytes might contribute to their impaired migration via resistance to shape change either by: (1) contributing

to changes in membrane tension (which is determined not only by local membrane-cortex attachment, but also by such attachment elsewhere in the cell<sup>22</sup>); or (2) affecting global resistance to shape change (because of the extended arc of membrane-associated ezrin there).

The present studies identify phospho-ERM as a major regulator of lymphocyte membrane tension, migration, and transmigration. There are probably additional regulators of membrane tension in lymphocytes that we predict will also regulate lymphocyte migration. Class I myosins are excellent candidates because they resemble ERM proteins in: linking actin cytoskeleton to plasma membrane, regulating membrane tension and/or local deformability in various cell types or unicellular organisms,<sup>28,48-50</sup> and influencing cell migration in *Dictyostelium discoideum*.<sup>50</sup>

## Acknowledgments

The authors thank Andrew Doyle, Lionel Feigenbaum, Jeffrey Hammer, Hyun Park, Genevieve Sanchez, and David Winkler for assistance and discussion.

This work was supported by the intramural programs of National Human Genome Research Institute and National Cancer Institute. M.J.T. and R.N. were supported by the National Institutes of Health (R01-DK075555) and the American Heart Association (grant-in-aid 09GRNT2310188 and postdoctoral fellowship 0825358E).

## Authorship

Contribution: Y.L., N.V.B., C.P., R.N., S.M.L., G.P.-L., K.B.-A., and H.Q. performed the research; Y.L. and S.S. wrote the manuscript; and all authors conceptualized experiments, analyzed the data, and reviewed/edited the manuscript.

Conflict-of-interest disclosure: The authors declare no competing financial interests.

The current affiliation for H.Q. is School of Medicine, Tsinghua University, Beijing, People's Republic of China.

Correspondence: Stephen Shaw, National Institutes of Health, 10 Center Dr, MSC 1360, Bldg 10, Rm 4B36, Bethesda, MD 20892; e-mail: shaws@mail.nih.gov.

## References

- Campbell DJ, Kim CH, Butcher EC. Chemokines in the systemic organization of immunity. *Immunol Rev*. 2003;195:58-71.
- Luster AD, Alon R, von Andrian UH. Immune cell migration in inflammation: present and future therapeutic targets. *Nat Immunol*. 2005;6(12):1182-1190.
- Ley K, Laudanna C, Cybulsky MI, Nourshargh S. Getting to the site of inflammation: the leukocyte adhesion cascade updated. *Nat Rev Immunol*. 2007;7(9):678-689.
- Fehon RG, McClatchey AI, Bretscher A. Organizing the cell cortex: the role of ERM proteins. *Nat Rev Mol Cell Biol*. 2010;11(4):276-287.
- Niggli V, Rossy J. Ezrin/radixin/moesin: versatile controllers of signaling molecules and of the cortical cytoskeleton. *Int J Biochem Cell Biol*. 2008;40(3):344-349.
- Fievat BT, Gautreau A, Roy C, et al. Phosphoinositide binding and phosphorylation act sequentially in the activation mechanism of ezrin. *J Cell Biol*. 2004;164(5):653-659.
- Hao JJ, Liu Y, Kruhlak M, Debell KE, Rellahan BL, Shaw S. Phospholipase C-mediated hydrolysis of PIP2 releases ERM proteins from lymphocyte membrane. *J Cell Biol*. 2009;184(3):451-462.
- Nakamura F, Amieva MR, Furthmayr H. Phosphorylation of threonine 558 in the carboxyl-terminal actin-binding domain of moesin by thrombin activation of human platelets. *J Biol Chem*. 1995;270(52):31377-31385.
- Brown MJ, Nijhara R, Hallam JA, et al. Chemokine stimulation of human peripheral blood T-lymphocytes induces rapid dephosphorylation of ERM proteins, which facilitates loss of microvilli and polarization. *Blood*. 2003;102(12):3890-3899.
- Yoshinaga-Ohara N, Takahashi A, Uchiyama T, Sasada M. Spatiotemporal regulation of moesin phosphorylation and rear release by Rho and serine/threonine phosphatase during neutrophil migration. *Exp Cell Res*. 2002;278(1):112-122.
- Huang L, Wong TY, Lin RC, Furthmayr H. Replacement of threonine 558, a critical site of phosphorylation of moesin in vivo, with aspartate activates F-actin binding of moesin: regulation by conformational change. *J Biol Chem*. 1999;274(18):12803-12810.
- Gautreau A, Louvard D, Arpin M. Morphogenic effects of ezrin require a phosphorylation-induced transition from oligomers to monomers at the plasma membrane. *J Cell Biol*. 2000;150(1):193-203.
- Polesello C, Delon I, Valenti P, Ferrer P, Payre F. Dmoesin controls actin-based cell shape and polarity during *Drosophila melanogaster* oogenesis. *Nat Cell Biol*. 2002;4(10):782-789.
- Dard N, Louvet-Vallée S, Santa-Maria A, Maro B. Phosphorylation of ezrin on threonine T567 plays a crucial role during compaction in the mouse early embryo. *Dev Biol*. 2004;271(1):87-97.
- Lee JH, Katakai T, Hara T, Gonda H, Sugai M, Shimizu A. Roles of p-ERM and Rho-ROCK signaling in lymphocyte polarity and uropod formation. *J Cell Biol*. 2004;167(2):327-337.
- Li Y, Harada T, Juang YT, et al. Phosphorylated ERM is responsible for increased T cell polarization, adhesion, and migration in patients with systemic lupus erythematosus. *J Immunol*. 2007;178(3):1938-1947.



17. Belkina NV, Liu Y, Hao JJ, Karasuyama H, Shaw S. LOK is a major ERM kinase in resting lymphocytes and regulates cytoskeletal rearrangement through ERM phosphorylation. *Proc Natl Acad Sci U S A*. 2009;106(12):4707-4712.
18. Parameswaran N, Matsui K, Gupta N. Conformational switching in ezrin regulates morphological and cytoskeletal changes required for B cell chemotaxis. *J Immunol*. 2011;186(7):4088-4097.
19. Roch F, Polesello C, Roubinet C, et al. Differential roles of PtdIns(4,5)P2 and phosphorylation in moesin activation during *Drosophila* development. *J Cell Sci*. 2010;123(12):2058-2067.
20. Suda J, Zhu L, Karvar S. Phosphorylation of radixin regulates cell polarity and Mrp-2 distribution in hepatocytes. *Am J Physiol Cell Physiol*. 2011;300(3):C416-C424.
21. Kunda P, Pelling AE, Liu T, Baum B. Moesin controls cortical rigidity, cell rounding, and spindle morphogenesis during mitosis. *Curr Biol*. 2008;18(2):91-101.
22. Sheetz MP, Dai J. Modulation of membrane dynamics and cell motility by membrane tension. *Trends Cell Biol*. 1996;6(3):85-89.
23. Dai J, Ting-Beall HP, Sheetz MP. The secretion-coupled endocytosis correlates with membrane tension changes in RBL 2H3 cells. *J Gen Physiol*. 1997;110(1):1-10.
24. Apodaca G. Modulation of membrane traffic by mechanical stimuli. *Am J Physiol Renal Physiol*. 2002;282(2):F179-F190.
25. Togo T, Krasieva TB, Steinhart RA. A decrease in membrane tension precedes successful cell-membrane repair. *Mol Biol Cell*. 2000;11(12):4339-4346.
26. Raucher D, Sheetz MP. Cell spreading and lamellipodial extension rate is regulated by membrane tension. *J Cell Biol*. 2000;148(1):127-136.
27. Sheetz MP. Cell control by membrane-cytoskeleton adhesion. *Nat Rev Mol Cell Biol*. 2001;2(5):392-396.
28. Nambiar R, McConnell RE, Tyska MJ. Control of cell membrane tension by myosin-I. *Proc Natl Acad Sci U S A*. 2009;106(29):11972-11977.
29. Diz-Munoz A, Krieg M, Bergert M, et al. Control of directed cell migration in vivo by membrane-to-cortex attachment. *PLoS Biol*. 2010;8(11):e1000544.
30. Ilani T, Khanna C, Zhou M, Veenstra TD, Bretscher A. Immune synapse formation requires ZAP-70 recruitment by ezrin and CD43 removal by moesin. *J Cell Biol*. 2007;179(4):733-746.
31. Shaffer MH, Dupree RS, Zhu P, et al. Ezrin and moesin function together to promote T cell activation. *J Immunol*. 2009;182(2):1021-1032.
32. Schumacher KR, Popel AS, Anvari B, Brownell WE, Spector AA. Computational analysis of the tether-pulling experiment to probe plasma membrane-cytoskeleton interaction in cells. *Phys Rev E Stat Nonlin Soft Matter Phys*. 2009;80(4):041905.
33. Xu G, Shao JY. Human neutrophil surface protrusion under a point load: location independence and viscoelasticity. *Am J Physiol Cell Physiol*. 2008;295(5):C1434-C1444.
34. Hochmuth FM, Shao JY, Dai J, Sheetz MP. Deformation and flow of membrane into tethers extracted from neuronal growth cones. *Biophys J*. 1996;70(1):358-369.
35. Serrador JM, Alonso-Lebrero JL, del Pozo MA, et al. Moesin interacts with the cytoplasmic region of intercellular adhesion molecule-3 and is redistributed to the uropod of T-lymphocytes during cell polarization. *J Cell Biol*. 1997;138(6):1409-1423.
36. Kishimoto TK, Jutila MA, Berg EL, Butcher EC. Neutrophil Mac-1 and MEL-14 adhesion proteins inversely regulated by chemotactic factors. *Science*. 1989;245(4923):1238-1241.
37. Park EJ, Peixoto A, Imai Y, et al. Distinct roles for LFA-1 affinity regulation during T-cell adhesion, diapedesis, and interstitial migration in lymph nodes. *Blood*. 2010;115(8):1572-1581.
38. Semmrich M, Smith A, Feterowski C, et al. Importance of integrin LFA-1 deactivation for the generation of immune responses. *J Exp Med*. 2005;201(12):1987-1998.
39. Park EJ, Mora JR, Carman CV, et al. Aberrant activation of integrin alpha4beta7 suppresses lymphocyte migration to the gut. *J Clin Invest*. 2007;117(9):2526-2538.
40. Smith DF, Deem TL, Bruce AC, Reutershan J, Wu D, Ley K. Leukocyte phosphoinositide-3 kinase  $\gamma$  is required for chemokine-induced, sustained adhesion under flow in vivo. *J Leukoc Biol*. 2006;80(6):1491-1499.
41. Gakidis MA, Cullere X, Olson T, et al. Vav GEFs are required for beta2 integrin-dependent functions of neutrophils. *J Cell Biol*. 2004;166(2):273-282.
42. Mocsai A, Zhou M, Meng F, Tybulewicz VL, Lowell CA. Syk is required for integrin signaling in neutrophils. *Immunity*. 2002;16(4):547-558.
43. Brambilla D, Fais S. The Janus-faced role of ezrin in "linking" cells to either normal or metastatic phenotype. *Int J Cancer*. 2009;125(10):2239-2245.
44. Hao JJ, Wang G, Pisitkun T, et al. Enrichment of distinct microfilament-associated and GTP-binding-proteins in membrane/microvilli fractions from lymphoid cells. *J Proteome Res*. 2008;7(7):2911-2927.
45. Faure S, Salazar-Fontana LI, Semichon M, et al. ERM proteins regulate cytoskeleton relaxation promoting T cell-APC conjugation. *Nat Immunol*. 2004;5(3):272-279.
46. Fackler OT, Grosse R. Cell motility through plasma membrane blebbing. *J Cell Biol*. 2008;181(6):879-884.
47. Lorentzen A, Bamber J, Sadok A, Elson-Schwab I, Marshall CJ. An ezrin-rich, rigid uropod-like structure directs movement of amoeboid blebbing cells. *J Cell Sci*. 2011;124(8):1256-1267.
48. Dai J, Ting-Beall HP, Hochmuth RM, Sheetz MP, Titus MA. Myosin I contributes to the generation of resting cortical tension. *Biophys J*. 1999;77(2):1168-1176.
49. Olety B, Walte M, Honnert U, Schillers H, Bahler M. Myosin 1G (Myo1G) is a haematopoietic specific myosin that localises to the plasma membrane and regulates cell elasticity. *FEBS Lett*. 2010;584(3):493-499.
50. Novak KD, Titus MA. Myosin I overexpression impairs cell migration. *J Cell Biol*. 1997;136(3):633-647.